Journal of Sound and Vibration 329 (2010) 4950–4969

Contents lists available at ScienceDirect

Journal of Sound and Vibration

journal homepage: www.elsevier.com/locate/jsvi

Linear and nonlinear vibrations analysis of viscoelastic sandwich beams

M. Bilasse [a], E.M. Daya [a], L. Azrar [b,*]

[a] Laboratoire de Physique et Mécanique des Matériaux, FRE CNRS 3236, Université Paul Verlaine-Metz, Ile du Saulcy, 57045 Metz Cedex 01, France
[b] Equipe de Modélisation Mathématique et Contrôle, Département de Mathématiques, Faculté des Sciences et Techniques de Tanger, Université Abdelmalek Essaadi, BP 416 Tanger, Morocco

ARTICLE INFO

Article history:
Received 5 February 2010
Received in revised form
13 June 2010
Accepted 13 June 2010
Handling Editor: L.N. Virgin

ABSTRACT

In this paper, numerical models are proposed for linear and nonlinear vibrations analyses of viscoelastic sandwich beams with various viscoelastic frequency dependent laws using the finite element based solution. Real and various complex eigenmodes approaches are investigated as Galerkin bases. Based on harmonic balance method, simplified and general approaches are developed for nonlinear vibration analysis. Analytical frequency–amplitude and phase–amplitude relationships are elaborated based on the numerically computed complex eigenmodes. The equivalent loss factors and frequencies as well as the forced harmonic response and phase curves are performed for sandwich beams with various boundary conditions and frequency dependent viscoelastic laws.

1. Introduction

Viscoelastically damped structures find their application in many fields of engineering such as aerospace, aeronautics, automotive, naval construction and civil engineering. They are used for efficient noise reduction and vibration control. Classically viscoelastic damped structures are sandwich composites in which a soft viscoelastic layer is sandwiched between two stiff elastic ones. For lightweight and flexible structures, the sandwich with a viscoelastic core is very effective in controlling and reducing vibration responses [1,2]. For these structures, the damping results from a shearing in the viscoelastic core due to the difference between in-plane displacement of the elastic faces and the low stiffness of the core. This kind of structures finds much research interests during the last two decades. Many investigations have been devoted to the linear dynamic analysis and a review on the evolution of modeling passive damping were given in [3]. From an engineering point of view, the most relevant quantity is the equivalent frequency and loss factor associated with each vibration mode. Thus, many analytical and numerical methods have been presented to predict these structural damping properties in the linear framework. They differ from each other depending on the computational cost and their ability to account for frequency dependence of the viscoelastic material. A review of applied methods can be found in [4].

It is well known that a large vibration amplitude may induce a dynamic behavior that differs significantly from the behavior predicted by the linear theories. Multimodal approach, iterative-incremental procedures or the asymptotic numerical method can be used for the nonlinear response and lead the solution in a large frequency range. These procedures are developed for elastic and undamped beams, plates and shells with the geometrical nonlinearity effect [5–9]. For viscoelastically damped structures, the nonlinear geometrical effect and the nonlinear frequency dependence of the stiffness effect have to be both considered. This leads to a complex problem to deal with. Unfortunately, there is only a

* Corresponding author.
E-mail addresses: l.azrar@uae.ma, azrarlahcen@yahoo.fr (L. Azrar).

0022-460X/$ - see front matter © 2010 Elsevier Ltd. All rights reserved.
doi:10.1016/j.jsv.2010.06.012

few works dealing with nonlinear vibrations of damped structures. Kovac et al. [10] and Hyer et al. [11] investigated theoretical and experimental nonlinear forced responses of a clamped three layered sandwich beam. Iu et al. [12,13] analyzed the nonlinear vibrations of multilayered sandwich beams based on incremental harmonic balance method and finite element. The nonlinear free vibrations of damped sandwich plates and cylindrical panels have been investigated by Xia and Lukaziewicz [14,15] using harmonic balance method and a multimode Galerkin's procedure. Ganapathi et al. [16] highlighted the variation of damping characteristics with aspect ratio of sandwich beams in conjunction with thickness ratio of skin-to-core and material properties. In all these studies, only the constant complex modulus is used for the viscoelastic core. More recently, Daya et al. [17,18] and Boutyour et al. [19] presented an elementary theory for nonlinear vibrations of damped sandwich structures. The presented theory was applied analytically and numerically to viscoelastic sandwich beams, plates and shells. Frequency–amplitude relationships depending on three coefficients are obtained by means of one mode Galerkin's procedure and the harmonic balance method. This permits to easily characterize the evolution of the equivalent loss factor and the nonlinear frequency with the vibration amplitude. However, the model presented in [17,19] for nonlinear vibrations analysis of damped sandwich structures was performed using real eigenmodes as Galerkin's basis and assuming that the variation of the nonlinear response has the same shape as the linear one. Real eigenmodes remain an approximation in the analysis of nonlinear vibrations of viscoelastic structures and especially for highly damped structures. Furthermore, no survey on the limit and validity range of the real eigenmodes approximation is available in the literature. There is still a need for numerical assessment to raise a clear picture on the applicability and the accuracy of real eigenmodes approximation with respect to the complex eigenmodes approximation for linear and nonlinear vibrations analysis of damped sandwich structures. In this paper, a numerical method for linear and nonlinear vibrations analysis of viscoelastically damped sandwich beams is developed with a finite element based solution. This method couples the harmonic balance technique to one mode Galerkin's procedure. A general formulation taking into account the frequency dependent viscoelastic behavior is presented. Real modes, improved real modes, approached complex modes and exact complex modes are used for linear and nonlinear vibrations characteristics of viscoelastic sandwich beams with various boundary conditions. The accuracy of the obtained results is deeply discussed for constant and various frequency dependent viscoelastic core properties.

2. Mathematical formulation

In this paper, the viscoelastic sandwich beam model [17] with geometrical nonlinearities and zig–zag kinematic effects is used to get the governing equations of the linear and nonlinear vibrations analysis. For the finite element numerical solutions, the variational formulation is given. The convolution viscoelastic modeling is used in order to take into account the viscoelastic effect in a general way.

2.1. Viscoelastic sandwich structure

Let us consider a symmetric sandwich beam with a rectangular cross-section consisting of a viscoelastic layer sandwiched between two elastic layers as presented in Fig. 1. The coordinates x along the length, y along the width and z along the thickness directions are considered. One denotes by z_i the ith middle plane coordinate with respect to $z=0$ where the subscripts $i=1,3$ refer to the external faces while subscript $i=2$ refers to the core layer. The thickness of the face layers is h_f and of the viscoelastic core is h_c. The beam length in the x direction is L while the width in the y direction is b. The damping of the structure is assumed to be induced thanks to the shearing in the viscoelastic core layer. The following assumptions are used:

- plane transverse sections to the middle plane remain plane after bending,
- the three layers undergo the same transverse deflection,
- no slipping occurs at the interfaces between the three layers,
- the constitutive materials of the beam are linear homogeneous and isotropic.

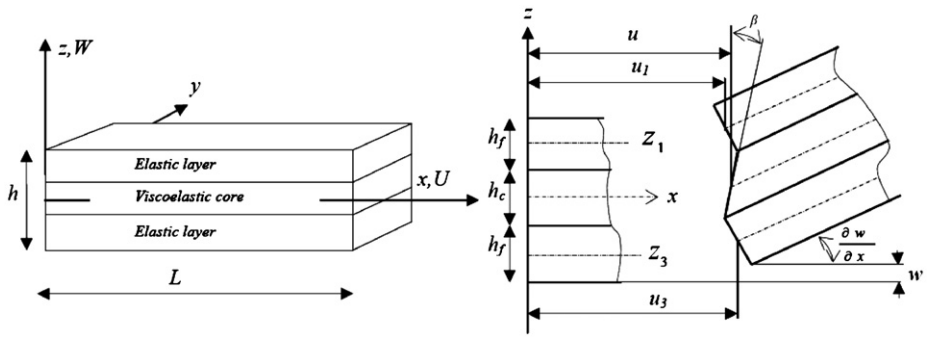

Fig. 1. Sandwich beam's configuration.

The kinematic properties are described based on the classical Euler–Bernoulli's beam theory for the elastic face layers and on the Timoshenko's beam theory for the viscoelastic layer. The face layers have the same thickness, mass density and Young's/shear modulus. The core material is linearly viscoelastic with a complex frequency dependent Young's/shear modulus, but the Poisson ratio is assumed to be real constant. Geometrical nonlinearity effects are introduced using the Von Karman's theory which assumes moderate rotations. Based on these assumptions, the strain and displacement fields and the constitutive laws governing the viscoelastic sandwich beam motion can be derived as reported in the Appendix A.

2.2. Variational formulation

The virtual work principle is applied to establish the equation of motion of the sandwich beam subjected to a transverse harmonic excitation force $F(x,t)$. The longitudinal and rotatory inertia effects are disregarded and only the transverse inertia effect is considered. The interfaces displacement continuity, expressed in the Appendix A leads to the generalized displacement vector $\{u,w,\beta\}$ related to the core layer. Thus for the viscoelastic sandwich beam, the three components of the virtual work principle are [17]

$$\delta P_{\text{int}} = -\int_0^L \{N(\delta u' + w'\delta w') + M_\beta \delta\beta' + M_w \delta w'' + T(\delta w' + \delta\beta)\}\,\mathrm{d}x$$

$$\delta P_{\text{ext}} = \int_0^L F\delta w\,\mathrm{d}x$$

$$\delta P_{\text{acc}} = (2\rho_f S_f + \rho_c S_c)\int_0^L \ddot{w}\delta w\,\mathrm{d}x \tag{1}$$

where δP_{int} represents the virtual work of the internal forces which is obtained by assembling the virtual work equations of the three layers, δP_{ext} the virtual work of the external loads and δP_{acc} the virtual work of the kinetic energy. δu, δw and $\delta\beta$ are components of the virtual displacement vector. ρ_f and ρ_c are mass density of the faces and of the core, respectively. The notations (g',g'') and $(\dot{g},\ddot{g})$ stand for the spatial derivatives $(\partial g/\partial x,\partial^2 g/\partial x^2)$ and temporal derivatives $(\partial g/\partial t,\partial^2 g/\partial t^2)$, respectively. Referring to Eq. (1), the internal forces involved in the virtual work equations are [17]

$$N = N_1 + N_2 + N_3$$

$$T = \frac{S_c}{2(1+v_c)} Y * (\dot{w}' + \dot{\beta})$$

$$M_\beta = M_2 + (N_1 - N_3)\frac{h_c}{2}$$

$$M_w = M_1 + M_3 + (N_3 - N_1)\frac{h_f}{2} \tag{2}$$

in which N is the axial force, T the shear force, M_β and M_w are the bending moments in the whole beam while N_i and M_i are the axial force and bending moment of each layer i as listed in the Appendix A. The governing equations of motion of the viscoelastic sandwich beam is given by

$$-\delta P_{\text{int}} = \delta P_{\text{ext}} - \delta P_{\text{acc}}$$

$$\int_0^L \{N\delta u' + Nw'\delta w' + M_\beta\delta\beta' + M_w\delta w'' + T(\delta w' + \delta\beta)\}\,\mathrm{d}x = \int_0^L F\delta w\,\mathrm{d}x - (2\rho_f S_f + \rho_c S_c)\int_0^L \ddot{w}\delta w\,\mathrm{d}x \tag{3}$$

Note that Eq. (3) shows a coupling between flexural and membrane effects. As the axial inertia terms and the axial excitation force are disregarded, the axial equilibrium solution can be obtained by

$$\int_0^L N\delta u'\,\mathrm{d}x = 0 \tag{4}$$

The flexural response of the viscoelastic sandwich beam can be then investigated by solving the following equation:

$$\int_0^L \{Nw'\delta w' + M_\beta\delta\beta' + M_w\delta w'' + T(\delta w' + \delta\beta)\}\,\mathrm{d}x = \int_0^L F\delta w\,\mathrm{d}x - (2\rho_f S_f + \rho_c S_c)\int_0^L \ddot{w}\delta w\,\mathrm{d}x \tag{5}$$

The finite element method will be used for the numerical discretization of this equation. Note that this equation is a nonlinear integro-partial differential equation. As there is no analytical solution of this equation, only approximated solutions will be investigated. The Galerkin's approach will be used based on real, improved real, approached complex and exact complex eigenmodes. The real, improved real and approached complex eigenmodes are obtained by solving eigenvalue problems and the exact complex eigenmodes will be obtained by an asymptotic numerical method.

3. Linear vibrations analysis

In the present section, the linear free vibrations of the viscoelastic sandwich beams are investigated based on the finite element method. The material properties of the viscoelastic core are frequency dependent in order to take into account various viscoelastic laws.

3.1. Finite element matrix formulation

To get the vibration eigenmodes, frequencies and equivalent loss factors, one must solve the flexural problem Eq. (5) in the linear framework:

$$\int_0^L \{M_\beta \delta\beta' + M_w \delta w'' + T(\delta w' + \delta\beta)\}\,\mathrm{d}x = -(2\rho_f S_f + \rho_c S_c)\int_0^L \ddot{w}\delta w\,\mathrm{d}x \tag{6}$$

For free vibrations analysis, the solution is sought in the following harmonic form:

$$\left\{\begin{array}{l} w(x,\quad t) \\ \beta(x,\quad t)\end{array}\right\} = \left\{\begin{array}{l} W(x) \\ B(x)\end{array}\right\} \mathrm{e}^{\mathrm{i}\omega t} \tag{7}$$

The finite element method is applied to discretize the flexural problem (6). One dimensional two nodes finite element is used in this paper. Each node has three degrees of freedom (DOF) which describe the transverse displacement (W), the slope ($\partial W/\partial x$) and the rotation (B). Thus, for each element bounded by the nodes 1 and 2, the nodal displacement vector is

$$\{U^e\} = {}^T[W_1 \;\; W'_1 \;\; B_1 \;\; W_2 \;\; W'_2 \;\; B_2] \tag{8}$$

Using classical polynomial shape functions [20], the element displacement field vector is written as

$$\left\{\begin{array}{l} W \\ B\end{array}\right\} = \left[\begin{array}{c} N_w \\ N_\beta\end{array}\right]\{U^e\} \tag{9a}$$

$$[N_w] = [n_1(\xi) \;\; n_2(\xi) \;\; 0 \;\; n_3(\xi) \;\; n_4(\xi) \;\; 0] \tag{9b}$$

$$[N_\beta] = [0 \;\; 0 \;\; n_5(\xi) \;\; 0 \;\; 0 \;\; n_6(\xi)] \tag{9c}$$

where $[N_w]$ and $[N_\beta]$ are the shape function matrices listed in the Appendix B. Inserting Eqs. (9) into Eq. (6), one gets the following elementary eigenvalue problem:

$$([K^e(\omega)] - \omega^2[M^e])\{U^e\} = 0 \tag{10}$$

where $[M^e]$ and $[K^e]$ are element mass and stiffness matrices, respectively, for which more detail is given in the Appendix B. These matrices are assembled to get the overall complex nonlinear eigenvalue problem:

$$([K(\omega)] - \omega^2[M])\{U\} = 0 \tag{11}$$

where $[M]$ and $[K]$ are the assembled mass and stiffness matrices, respectively, and $\{U\}$ the total displacement vector.

This matrix formulation is well known in the free vibrations analysis of viscoelastic structures [4,21–25]. Let us note that the problem (11) cannot be solved by the classical eigenvalue procedures when $[K]$ depends nonlinearly on ω. Many attempts have been proposed in the literature. The modal strain energy method [24] is applicable for frequency dependent structures but in some practical cases the error can be relatively large [26]. The direct frequency response method was applied in [25], but the high computational cost being its main drawback. The asymptotic approach [21] and the complex eigenvalue method [27] are limited to the case of constant stiffness viscoelastic structures. Other numerical methods for nonlinear eigenvalue problems [4,22,23,28] accounting the frequency dependence have been proved efficient to solve the problem (11) i.e: the asymptotic numerical algorithms [4,22], the order-reduction iterative algorithm [23] and the Arnoldi iterative projection method [28], but are not available in the existing commercial codes. More recently, a toolbox has been designed with the help of automatic differentiation techniques to make the asymptotic numerical method generic and easy of use [29–31]. The solution can be performed easily and in an exact way whatever the dependence on frequency of the matrix [K]. The exact complex eigenmodes are investigated based on this procedure.

3.2. Eigenmodes

The aim of this paper is the modeling and numerical investigation of the linear and nonlinear vibrations characteristics and behaviors of viscoelastic sandwich beams with various viscoelastic frequency dependent laws. As the Galerkin's approach will be used, an efficient basis is needed for accurate results and particularly for the nonconstant laws.

- *Real eigenmodes: RM.* For real eigenmodes, which are classically used in the modal strain energy method and conventionally by most authors, the real eigenvalue problem that corresponds to the delayed elasticity is solved using

eigenvalue problem algorithms such as subspace iteration or Lanczos method:

$$([K(0)]-\omega_0^2[M])\{U_0\}=0 \tag{12}$$

The nth natural frequency ω_{0_n} and the associated eigenmode $\{U_{0_n}\}$ numerically obtained are real quantities.

• *Improved real eigenmodes: IRM*. The real eigenmodes obtained by solving (12) are conventionally used and lead to accurate results for constant viscoelastic laws. Unfortunately, for frequency dependent laws these modes may lead to erroneous prediction of the equivalent frequencies and loss factors in the modal strain energy framework. To overcome this drawback, the following improved real eigenmodes procedure is introduced. Eq. (12) has to be solved to get ω_0. The improved real eigenmodes are then solutions of the following eigenproblem:

$$(Re[K(\omega_0)]-\omega_0^{\mathrm{imp}^2}[M])\{U_0^{\mathrm{imp}}\}=0 \tag{13}$$

in which $Re[K(\omega_0)]$ is the real part of $[K(\omega_0)]$, $\omega_{0_n}^{\mathrm{imp}}$ and $U_{0_n}^{\mathrm{imp}}$ are the nth improved eigenfrequencies and real eigenmodes. Note that Eqs. (12) and (13) are only identical for constant complex viscoelastic laws.

• *Approached complex eigenmodes: ACM*. The eigenvalue problem (11) must be solved in a way taking into account the frequency dependence introduced by the viscoelastic law. Thus, the stiffness matrix $[K(\omega)]$ is approximated around the real frequency ω_0 that yields the following complex eigenvalue problem:

$$([K(\omega_0)]-\omega^2[M])\{U\}=0 \tag{14}$$

Solving this complex eigenvalue problem leads to the nth frequencies ω_n and eigenmodes $\{U_n\}=\{U(\omega_{0_n})\}$ which are complex quantities.

• *Exact complex eigenmodes: ECM*. The asymptotic numerical method (ANM) is used to solve the nonlinear problem (11) without any approximation. Setting $\lambda=\omega^2$, the solution (U,λ) can be represented by power series with respect to a path parameter p [4,30,31]:

$$\begin{aligned} U &= U_0+pU_1+p^2U_2+p^3U_3+\cdots+p^jU_j+\cdots,\\ \lambda &= \lambda_0+p\lambda_1+p^2\lambda_2+p^3\lambda_3+\cdots+p^i\lambda_j+\cdots \end{aligned} \tag{15}$$

in which U_j and λ_j are new unknowns which have to be computed. Introducing Eq. (15) into Eq. (11) and equating like powers of p leads to a set of linear problems. The so called *diamant approach* [29] couples the ANM and the automatic differentiation (AD) techniques automating the computations of higher order derivatives. To that end, an AD toolbox has been designed [30] and the nonlinear problem (11) can therefore be solved in an efficient and generic form using the ANM solver presented in [31]. Applied to the present problem, it consists of splitting the residual equation (11) in two sub-residues:

$$\begin{aligned} R(U,\lambda) &= ([K(0)]+E(\lambda)[K_v]-\lambda[M])\{U\}=S(U,\lambda)+T(U,\lambda)=0\\ S(U,\lambda) &= ([K(0)]-\lambda[M])\{U\}\\ T(U,\lambda) &= E(\lambda)[K_v]\{U\} \end{aligned} \tag{16}$$

where $E_v(\lambda)=E(\lambda)+E_v(0)$ is a complex nonlinear function describing the dependence on frequency of the Young's/shear modulus of the viscoelastic material and $[K_v]$ is a purely real matrix. The homotopy technique [31–33] is used to deform the original problem by introducing the path parameter p in order to drive the solution from the real eigenvalue problem $S(U,\lambda)=0$ whose solution (U_0,λ_0) is known to the complex one

$$R(U,\lambda,p)=S(U,\lambda)+pT(U,\lambda)=0,\quad p\in[0\ \ 1] \tag{17}$$

Inserting the Taylor series S_j and T_j of functions S and T into Eq. (17) allows to deduce the generic linear systems to be implemented with *diamant*. Applying the derivative propagation chain rules with suitable initialization leads to compute the unknowns (U_j,λ_j) in the generic form [31]:

$$\begin{bmatrix} A_0 & U_0\\ {}^TU_0 & 0 \end{bmatrix}\begin{Bmatrix} U_j\\ \kappa \end{Bmatrix}=\begin{Bmatrix} -\{S_{j|U_j=0}\}-p\{T_{j|U_j=0}\}-\{T_{j-1}\}\\ 0 \end{Bmatrix}$$

$$\lambda_j=-\frac{{}^TU_0[\{S_{j|U_j=0,\lambda_j=0}\}+p\{T_{j|U_j=0,\lambda_j=0}\}+T_{j-1}]}{{}^TU_0[\{S_{1|U_1=0,\lambda_1=1}\}+p\{T_{1|U_1=0,\lambda_1=1}\}]} \tag{18}$$

where the matrix $A_0=[K(0)]-\lambda_0[M]+pE(\lambda_0)[K_v]$, while κ denotes the Lagrange multiplier. The solution (U,λ) is then determined using the continuation procedure. Theoretical formulas and numerical aspects on the computation of the unknowns (U_j,λ_j) and the continuation procedure are detailed in Ref. [31] for convenience. Thus, to generate the solution of the problem (11), the user of the ANM solver has only to define the viscoelastic function E and the sub-residues S, T by providing the finite element matrices $[K(0)]$,$[K_v]$, $[M]$ and the starting guess (U_0,λ_0). The troncature order and the precision are also user-defined. The vector $\{U\}$ is the exact complex eigenmode while the eigenvalue λ is the square of the exact complex frequency ω.

The associated linear equivalent nth frequency Ω_{l_n} and loss factor η_{l_n} can be obtained by the following formulationship:

$$\omega_n^2 = \Omega_{l_n}^2(1+\mathrm{i}\eta_{l_n}) = \frac{{}^T\{\overline{U}_n\}[K(\omega_{0_n})]\{U_n\}}{{}^T\{\overline{U}_n\}[M]\{U_n\}} \tag{19}$$

Note that when the real mode is used, Eq. (19) is exactly the modal strain energy. Based on the other modes, the classical modal strain energy is improved and particularly for frequency dependent viscoelastic laws. These modes will be also used as a Galerkin's basis for the nonlinear vibrations analysis of the considered viscoelastic sandwich beam. As the one mode Galerkin's approach will be considered in this analysis, the previous real, improved real, approached complex and exact complex eigenmodes will be used. The validity of each eigenmode approach will be assessed in the linear and nonlinear analysis for various viscoelastic laws.

4. Nonlinear amplitude equation

In this paper, the analysis is limited to periodic responses to a transverse harmonic excitation $F(x,t)=f(x)\mathrm{e}^{\mathrm{i}\omega t}$ or to free vibrations. The beam response is assumed to be harmonic in time and almost parallel to a single linear vibration mode in space with an arbitrary complex amplitude. Based on the one mode Galerkin's approximation, the deflection and rotation functions are sought in the following form:

$$\begin{Bmatrix} w(x,\ t) \\ \beta(x,\ t) \end{Bmatrix} = A\begin{Bmatrix} W(x) \\ B(x) \end{Bmatrix}\mathrm{e}^{\mathrm{i}\omega t} + CC \tag{20}$$

where A is the complex unknown amplitude, and CC denotes the conjugate complex. The vector $\{W,B\}$ is the Galerkin's basis to be chosen which approximates the spatial variation of the vibration mode. $\{W,B\}$ is numerically computed using the previous eigenmodes approaches.

The explicit form of Eq. (5) is completely known if one carries out the axial affects induced by the axial force. Referring to Eq. (2), one can realize that the axial force $N(x,t)$ is function of the displacement field variables $\{u,w\}$. Using Eq. (20), the axial force $N(x,t)$ and the axial displacement $u(x,t)$ can be sought as functions of harmonics 0 and 2ω [17]:

$$\begin{aligned} u(x,t) &= |A|^2 u_0(x) + \{A^2 u_{2\omega}(x)\mathrm{e}^{\mathrm{i}2\omega t} + CC\} \\ N(x,t) &= |A|^2 N_0(x) + \{A^2 N_{2\omega}(x)\mathrm{e}^{\mathrm{i}2\omega t} + CC\} \end{aligned} \tag{21}$$

where u_0 and N_0 are the amplitudes of u and N, respectively, at the harmonic 0, as well as $u_{2\omega}$ and $N_{2\omega}$ at the harmonic 2ω. The notation $|\bullet|$ stands for the complex modulus. Inserting Eq. (21) into Eq. (2), and using Eqs. (44) and (45), one gets the amplitudes of the axial force:

$$\begin{aligned} N_0(x) &= (2E_fS_f + S_cE_c(0))(u'_0(x) + |W'(x)|^2) \\ N_{2\omega}(x) &= (2E_fS_f + S_cE_c(2\omega))(u'_{2\omega}(x) + \tfrac{1}{2}(W'(x))^2) \end{aligned} \tag{22}$$

Indeed, by taking account of Eq. (22) in Eq. (4), u_0 and $u_{2\omega}$ are solutions of the linear problems:

$$\begin{aligned} \int_0^L u'_0(x)\delta u'\,\mathrm{d}x &= -\int_0^L |W'(x)|^2\delta u'\,\mathrm{d}x \\ \int_0^L u'_{2\omega}(x)\delta u'\,\mathrm{d}x &= -\int_0^L \frac{1}{2}(W'(x))^2\delta u'\,\mathrm{d}x \end{aligned} \tag{23}$$

Applying the harmonic balance method and using the previous equations, one gets an equation for the complex amplitude [17]:

$$-\omega^2 mA + kA + k_{nl}\overline{A}A^2 = Q \tag{24}$$

where m, k, k_{nl} and Q are the modal mass, the linear modal stiffness, the nonlinear modal stiffness and the modal force, respectively. The notation $\overline{\bullet}$ stands for the conjugate complex:

$$\begin{aligned} m &= \int_0^L (2\rho_fS_f + \rho_cS_c)|W|^2\,\mathrm{d}x \\ k &= \int_0^L \frac{1}{2}\{(2I_cE_c(\omega) + E_fS_fh_c^2)|B'|^2 - E_fS_fh_fh_c(W''\overline{B}' + \overline{W}''B')\}\,\mathrm{d}x + \int_0^L \frac{1}{2}\{E_f(4I_f + S_fh_f^2)|W''|^2 + 2S_cG_c(\omega)|W' + B|^2\}\,\mathrm{d}x \\ k_{nl} &= \int_0^L (N_0|W'|^2 + N_{2\omega}\overline{W}'^2)\,\mathrm{d}x \\ Q &= \int_0^L f\overline{W}\,\mathrm{d}x \end{aligned} \tag{25}$$

All these coefficients can be computed using the finite element model proposed in Section 3.1. The analysis is conducted here for axially immovable sandwich beam ends and the corresponding reduced equations are given in the Appendix C. The amplitude equation is strongly nonlinear because the stiffnesses k and k_{nl} are frequency dependent through the Young's/shear modulus of the viscoelastic core:

$$k(\omega) = k^R(\omega) + \mathrm{i}k^I(\omega)$$

$$k_{nl}(\omega) = k_{nl}^R(\omega) + \mathrm{i}k_{nl}^I(\omega) \tag{26}$$

The solution can be sought in a restrictive way around the real frequency ω_0 or in a general case around any frequency ω.

4.1. Simplified approach

Assuming that the frequency ω is near the real frequency ω_0, the stiffnesses k and k_{nl} can be approximated around the real frequency, i.e: $k \approx k(\omega_0)$ and $k_{nl} \approx k_{nl}(\omega_0)$. Thus, for nonlinear free vibrations (Q=0), the nonlinear complex frequency is function of the amplitude $a = |A|$:

$$\omega^2 = \Omega_{nl}^2(1 + \mathrm{i}\eta_{nl}) \tag{27}$$

in which the nonlinear equivalent frequency Ω_{nl} and the nonlinear equivalent loss factor η_{nl} are deduced from the complex frequency [17]:

$$\begin{cases} \Omega_{nl}^2 = \Omega_l^2\left(1 + \left(\dfrac{a}{h}\right)^2 C^R(\omega_0)\right) \\ \eta_{nl} = \eta_l \dfrac{1 + \left(\dfrac{a}{h}\right)^2 C^I(\omega_0)}{1 + \left(\dfrac{a}{h}\right)^2 C^R(\omega_0)} \end{cases} \tag{28}$$

where $C^R(\omega_0) = h^2(k_{nl}^R(\omega_0)/k^R(\omega_0))$ and $C^I(\omega_0) = h^2(k_{nl}^I(\omega_0)/k^I(\omega_0))$ are non-dimensional modal coefficients introduced for the analysis. Both coefficients account for the nonlinear effects and characterize the amplitude dependence of the frequency and the loss factor. Writing the amplitude equation coefficients in the complex form $A = a\mathrm{e}^{\mathrm{i}\theta}$, $k = |k|\mathrm{e}^{\mathrm{i}\varphi}$, $k_{nl} = |k_{nl}|\mathrm{e}^{\mathrm{i}\psi}$, $Q = |Q|\mathrm{e}^{\mathrm{i}\alpha}$ leads to define the amplitude–frequency relationship $a(\omega)$ and the amplitude phase–frequency relationship $\theta(\omega)$:

$$|k_{nl}(\omega_0)|^2 a^6 + 2(k^R(\omega_0)k_{nl}^R(\omega_0) + k^I(\omega_0)k_{nl}^I(\omega_0) - \omega^2 m k_{nl}^R(\omega_0))a^4 + (|k(\omega_0)|^2 - 2\omega^2 m k^R(\omega_0) + \omega^4 m^2)a^2 = |Q|^2 \tag{29}$$

$$\tan(\theta - \alpha) = \frac{-k^I(\omega_0) - a^2 k_{nl}^I(\omega_0)}{-\omega^2 m + k^R(\omega_0) + a^2 k_{nl}^R(\omega_0)} \tag{30}$$

where $-\alpha$ represents the eigenmode's phase which is zero for real eigenmodes.

4.2. General approach

In the general case, the stiffnesses k and k_{nl} are not constant as assumed in the previous section and the amplitude equation must be solved in an exact way. Note that for the nth exact complex eigenmode $\{U_n\}$, the complex eigensolution ω_n of the nonlinear complex eigenvalue problem (11) satisfies

$$\omega_n^2 = \Omega_{l_n}^2(1 + \mathrm{i}\eta_{l_n}) = \frac{{}^T\{\overline{U}_n\}[K(\omega_n)]\{U_n\}}{{}^T\{\overline{U}_n\}[M]\{U_n\}} \tag{31}$$

which differs from the relationship (19) assuming that the damping properties are estimated around the real frequency ω_{0_n}. Thus the solution of the amplitude equation can be sought in a general framework in the vicinity of any frequency ω. Using the decomposition (26) in Eq. (24), the generalized amplitude equation is obtained

$$f_3(\omega)r^3 + f_2(\omega)r^2 + f_1(\omega)r + f_0 = 0 \tag{32}$$

where $r = a^2$, $f_0 = -|Q|^2$ and the functions $f_i(\omega)$ are given by

$$f_3(\omega) = k_{nl}^{R\,2}(\omega) + k_{nl}^{I\,2}(\omega)$$

$$f_2(\omega) = 2(k_{nl}^R(\omega)(-\omega^2 m + k^R(\omega)) + k^I(\omega)k_{nl}^I(\omega))$$

$$f_1(\omega) = (-\omega^2 m + k^R(\omega))^2 + k^{I\,2}(\omega) \tag{33}$$

For each fixed frequency ω, the solution can be performed using Sotta method for instance. As the conditions $(3f_3f_1 - f_2^2 \neq 0)$ and $(3f_0f_2 - f_1^2 \neq 0)$ are always satisfied for the considered frequencies ω, the three solutions of the cubic equation (32) are

given by

$$r_1(\omega)=\frac{\delta_1\delta^{1/3}-\gamma_1\gamma^{1/3}}{\delta_2\delta^{1/3}-\gamma_2\gamma^{1/3}}$$

$$r_2\omega)=\frac{\delta_1 j\delta^{1/3}-\gamma_1\gamma^{1/3}}{\delta_2 j\delta^{1/3}-\gamma_2\gamma^{1/3}}$$

$$r_3(\omega)=\frac{\delta_1 j^2\delta^{1/3}-\gamma_1\gamma^{1/3}}{\delta_2 j^2\delta^{1/3}-\gamma_2\gamma^{1/3}} \tag{34}$$

where

$$j=\mathrm{e}^{2i\pi/3}$$

$$\delta=\gamma_2^3 f_2+3\gamma_1\gamma_2^2 f_3$$

$$\gamma=\delta_2^3 f_2+3\delta_1\delta_2^2 f_3 \tag{35}$$

For the solution procedure, the coefficients $\delta_1,\delta_2,\gamma_1,\gamma_2$ are chosen in the way that the ratios δ_1/δ_2, γ_1/γ_2 be the roots of the associated Sotta resolvent equation:

$$(3f_3f_1-f_2^2)X^2+(9f_3f_0-f_2f_1)X+3f_2f_0-f_1^2=0 \tag{36}$$

Herein, numerical results are computed setting $\delta_2=\gamma_2=1$. Thus for each amplitude $a(\omega)$, the associated phase is

$$\tan(\theta-\alpha)=\frac{-k^I(\omega)-a^2k_{nl}^I(\omega)}{-\omega^2m+k^R(\omega)+a^2k_{nl}^R(\omega)} \tag{37}$$

Note that the peculiar case discussed in the previous section is recovered when setting $\omega=\omega_0$ in the stiffnesses k and k_{nl}.

5. Numerical results

For sake of clearness and effectiveness, the emphasis is on the linear and nonlinear vibrations of viscoelastic sandwich beams with various viscoelastic models. Numerical solutions are performed with a refined mesh size to ensure the convergence of the finite element method. Vibration characteristics and harmonic response and phase curves are provided for comparison that allow to assess the validity of each eigenmode approach.

5.1. Constant viscoelastic model

For the constant viscoelastic model, the viscoelastic properties of the core are introduced by a complex Young's modulus that is assumed to be constant:

$$E_c=E_0(1+i\eta_c) \tag{38}$$

where E_0 is the Young's modulus of the delayed elasticity and η_c the core's loss factor. This is the simplest and the classical way to take account the viscoelastic behavior. In such a case, the eigenvalue problem (11) becomes linear and can be solved directly. The proposed finite element is tested on the sandwich beam studied quite extensively in the literature [4,25,31,34]. Material and geometrical properties are given in Table 1. The equivalent frequencies and associated loss factors of the clamped–free sandwich beam corresponding to the first six modes are presented in Table 2 for different core's loss factors. These results are compared to the forced harmonic response results performed in [34] using the asymptotic numerical method (ANM) and the bandwidth approach and to those of [31] using the *diamant approach*. Note that both of the later references use complex eigenmodes. The same type of results performed with different eigenmodes approaches and the exact analytical formula of Rao [35] are given in Table 3 for the simply supported sandwich beam. In both tables, it is seen that for constant viscoelastic models, results obtained by the ACM approach and the ECM approach implemented with *diamant* are exactly the same. These results are quite the same of those provided by Rao's analytical formula [35] (Table 3) and closer to those of [34] using finite element method apart from slight differences observed for the equivalent frequencies (Table 2). This provides validation of the present finite element model. Tables 2 and 3 present that unlike for the ACM and the ECM approaches, the equivalent frequencies and associated loss factors remain constant for the RM approach whatever the core's loss factor. For small values of the core's loss factor such as 0.1 and 0.6, the equivalent frequencies and associated loss factors obtained by the ACM/ECM approach are closer to those obtained by the RM approach, but much differences are observed when the core's loss factor increases up to 1 and 1.5. In fact, the RM approach overestimates the equivalent loss factors and underestimates the equivalent frequencies. Thus for constant viscoelastic models, the ACM/ECM and RM approaches are equivalent only for small values of the core's loss factor.

Table 1
Material and geometrical properties of the sandwich beam.

Elastic faces	Young's modulus E_f=6.9 × 10^{10} N m^{-2} Poisson ratio $v_f = 0.3$ Density $\rho_f = 2766\,\mathrm{Kg\,m^{-3}}$ Thickness h_f=1.524 mm
Viscoelastic core	Young's modulus E_0=1.794 × 10^{6} N m^{-2} Poisson ratio $v_c = 0.3$ Density $\rho_c = 968.1\,\mathrm{Kg\,m^{-3}}$ Thickness h_c=0.127 mm
Beam	Length L=177.8 mm Width b=12.7 mm

Table 2
Linear equivalent frequencies and associated loss factors of the clamped–free sandwich beam for various core's loss factors.

η_c	RM		ACM		Bilasse et al. [31]		Abdoun et al. [34]	
	Ω_l (Hz)	η_l/η_c	Ω_l (Hz)	η_l/η_c	Ω_l (Hz)	η_l/η_c	Ω_l (Hz)	η_l/η_c
0.1	64.1	0.283	64.1	0.281	64.1	0.281	64.5	0.281
	296.6	0.243	296.6	0.242	296.7	0.242	298.9	0.242
	744.3	0.154	744.4	0.154	744.5	0.154	746.5	0.154
	1395.2	0.089	1395.6	0.088	1395.7	0.089	1407.7	0.089
	2263.4	0.057	2264.5	0.057	2264.5	0.057	2286.2	0.057
	3347.3	0.039	3349.7	0.039	3349.8	0.039	3385.7	0.039
0.6	64.1	0.283	65.5	0.246	65.5	0.246	65.9	0.247
	296.6	0.243	299.1	0.232	299.2	0.232	303.1	0.224
	744.3	0.154	746.2	0.152	746.3	0.153	752.3	0.150
	1395.2	0.089	1396.6	0.088	1396.6	0.089	1412.7	0.088
	2263.4	0.057	2265.1	0.057	2265.2	0.057	2290.6	0.057
	3347.3	0.039	3350.1	0.038	3350.2	0.039	3389.5	0.039
1	64.1	0.283	67.4	0.202	67.5	0.202	67.8	0.204
	296.6	0.243	303	0.217	303.1	0.218	309.1	0.201
	744.3	0.154	749.4	0.150	749.4	0.150	761.1	0.142
	1395.2	0.089	1397.9	0.088	1398.3	0.088	1420.6	0.086
	2263.4	0.057	2266.3	0.057	2266.3	0.057	2297.9	0.057
	3347.3	0.039	3350.9	0.038	3350.9	0.039	3395.9	0.037
1.5	64.1	0.283	69.9	0.153	69.9	0.153	70.3	0.155
	296.6	0.243	309.1	0.197	309.1	0.198	317.4	0.176
	744.3	0.154	755.2	0.145	755.2	0.146	777.2	0.131
	1395.2	0.089	1401.4	0.087	1401.4	0.087	1432.8	0.083
	2263.4	0.057	2268.4	0.056	2268.5	0.057	2310.1	0.056
	3347.3	0.039	3352.3	0.038	3352.3	0.039	3307.0	0.039

Fig. 2 displays the eigenmode deflection obtained by the ECM approach for the normalized sandwich beam under clamped–simple and clamped–free boundary conditions. The real and imaginary part have the same mode shape but differ in the amplitude depending on the damping. The imaginary part of the eigenmode which is commonly disregarded in the RM approach may become larger in the presence of high damping. In this case, the imaginary part cannot be neglected and complex eigenmodes are needed to take account accurately the whole damping induced in the structure.

The linear responses of the simply supported and the clamped–free sandwich beam corresponding to the first real and complex vibration mode are presented in Fig. 3 for different core's loss factors. Far from the resonance, the response obtained by the real mode and the one obtained by the complex mode are closer. But in the vicinity of the resonance, there is a shift between the real mode response and the complex mode response. In the resonance zone, the real mode underestimates the amplitude of the resonance peaks compared to the complex mode. The corresponding linear phases are displayed in Fig. 4 and the same observations are clearly shown. The shift between the real mode phase and the complex mode phase becomes larger when the damping increases, which proves that the RM approach is not suitable especially in the presence of high damping.

For the nonlinear vibrations analysis, the nonlinear modal coefficients C^R and C^I computed following the simplified approach (Section 4.1) are given in Table 4 for the sandwich beam under various boundary conditions. Recall that for the constant complex viscoelastic model, the RM approach is quite similar to the IRM approach and the ACM approach is quite

Table 3
Linear equivalent frequencies and associated loss factors of the simply supported sandwich beam for various core's loss factors.

η_c	RM		ACM		ECM		Rao's formula [35]	
	Ω_l (Hz)	η_l/η_c	Ω_l (Hz)	η_l/η_c	Ω_l (Hz)	η_l/η_c	Ω_l (Hz)	η_l/η_c
0.1	148.45	0.3507	148.51	0.3501	148.51	0.3502	148.51	0.3502
	488.45	0.1958	488.48	0.1958	488.48	0.1958	488.47	0.1958
	1034.73	0.1071	1034.75	0.1071	1034.75	0.1071	1034.69	0.1071
	1795.31	0.0652	1795.32	0.0652	1795.32	0.0652	1795.13	0.0653
	2771.97	0.0434	2771.98	0.0434	2771.98	0.0434	2771.49	0.0434
	3965.31	0.0308	3965.32	0.0308	3965.32	0.0308	3964.28	0.0308
0.6	148.45	0.3507	150.71	0.3328	150.71	0.3328	150.71	0.3329
	488.45	0.1958	489.76	0.1943	489.76	0.1943	489.75	0.1944
	1034.73	0.1071	1035.44	0.1069	1035.44	0.1069	1035.38	0.1069
	1795.31	0.0652	1795.74	0.0652	1795.74	0.0652	1795.54	0.0652
	2771.97	0.0434	2772.26	0.0434	2772.26	0.0434	2771.76	0.0434
	3965.31	0.0308	3965.51	0.0308	3965.51	0.0308	3964.47	0.0308
1	148.45	0.3507	154.43	0.3052	154.42	0.3052	154.42	0.3052
	488.45	0.1958	492.07	0.1918	492.07	0.1918	492.06	0.1918
	1034.73	0.1071	1036.69	0.1065	1036.69	0.1065	1036.63	0.1065
	1795.31	0.0652	1796.50	0.0651	1796.50	0.0651	1796.30	0.0651
	2771.97	0.0434	2772.76	0.0433	2772.76	0.0433	2772.27	0.0434
	3965.31	0.0308	3965.87	0.0308	3965.87	0.0308	3964.83	0.0308
1.5	148.45	0.3507	160.73	0.2627	160.72	0.2626	160.72	0.2626
	488.45	0.1958	496.50	0.1871	496.50	0.1870	496.49	0.1871
	1034.73	0.1071	1039.13	0.1059	1039.13	0.1059	1039.07	0.1059
	1795.31	0.0652	1797.98	0.0650	1797.98	0.0650	1797.78	0.0650
	2771.97	0.0434	2773.74	0.0433	2773.74	0.0433	2773.25	0.0433
	3965.31	0.0308	3966.56	0.0307	3966.56	0.0307	3965.52	0.0308

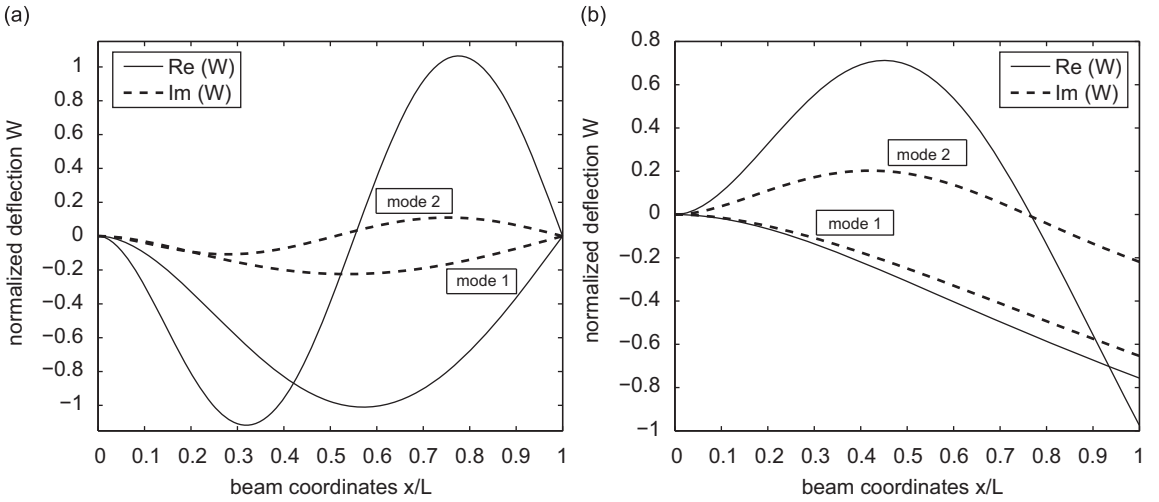

Fig. 2. Real and imaginary parts of the eigenmode deflection of the sandwich beam for $\eta_c = 1.5$ (a)C–S beam normalized at $x_0=L/2$ for the first mode and at $x_0=L/4$ for the second mode, (b) C–F beam normalized at $x_0=L$.

similar to the ECM approach. Unlike the ACM/ECM approach, the nonlinear modal coefficients remain constant for the RM/IRM approach whatever the core's loss factor.

5.2. Frequency dependent viscoelastic models

The vibration analysis of the viscoelastic sandwich beam of Table 1 is investigated for frequency dependent viscoelastic materials. The 3M ISD112 and the Polyvinyl-Butyral (PVB) viscoelastic materials are selected for the core. Based on the generalized Maxwell model, the frequency dependent shear modulus of the 3M ISD112, obtained by master curve fitting at

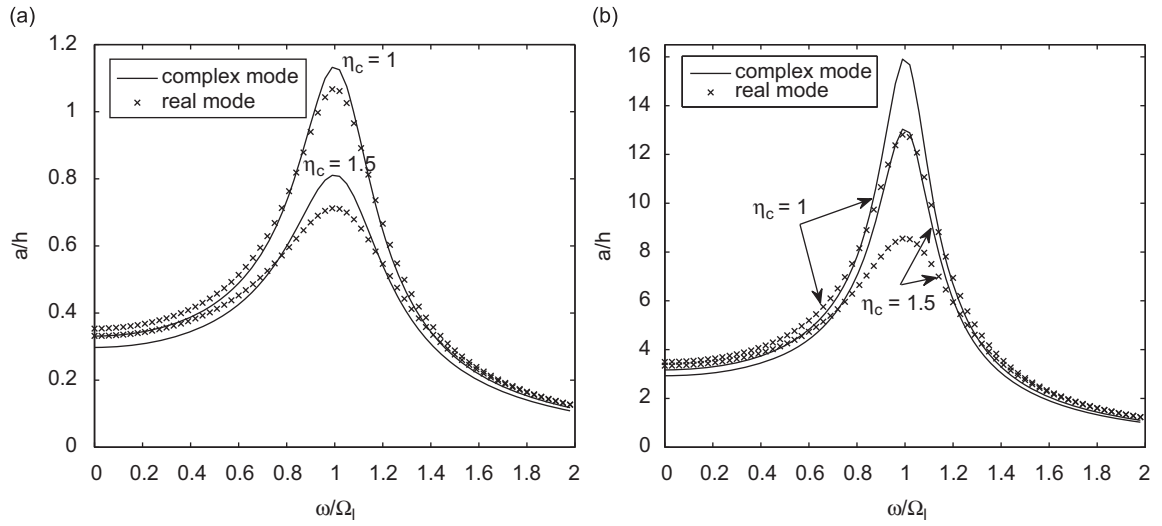

Fig. 3. Linear responses corresponding to the first real and complex vibration modes of the sandwich beam for various core's loss factors under a concentrated force f=10N at L/2 for S–S and at L for C–F. (a) Simply supported (S–S): $f(L/2)$=10N (b) clamped–free (C–F): $f|(L)$=10N.

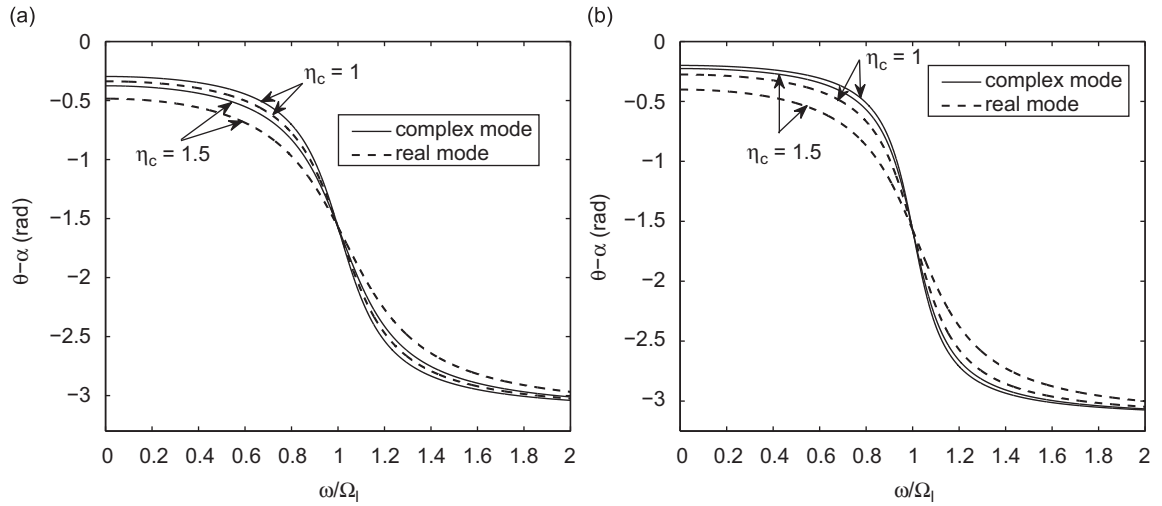

Fig. 4. Linear phases corresponding to the first real and complex vibration modes of the sandwich beam for various core's loss factors. (a) Simply supported (S–S) and (b) clamped–free (C–F).

the temperature 27 and 20 °C is given by [1,36]

$$G_c(\omega) = G_0\left(1+\sum_{j=1}^{3}\frac{\Delta_j\omega}{\omega-i\Omega_j}\right) \tag{39}$$

where G_0 is the shear modulus of the delayed elasticity and (Δ_j,Ω_j) are curve fitted-parameters given in Table 5. The mass density of the 3M ISD112 material [1] is $\rho_c = 1600\,\mathrm{Kg\,m^{-3}}$ and its Poisson ratio is $v_c = 0.5$. For the PVB viscoelastic material, its shear modulus may be represented at 20 °C by a power law [2]:

$$G_c(\omega) = G_\infty + (G_0 - G_\infty)[1+(i\omega\tau)^{1-\alpha}]^{-\beta} \tag{40}$$

where G_0=0.479 × 10^6 Pa is the delayed elasticity of the shear modulus, $G_\infty = 2.35 \times 10^8$ Pa, $\tau = 0.3979$, $\alpha = 0.46$ and $\beta = 0.1946$. The mass density of the PVB [2] is $\rho_c = 999\,\mathrm{Kg\,m^{-3}}$ and its Poisson ratio is $v_c = 0.4$. For frequency dependent viscoelastic models, the analysis is conducted first around the real frequency ω_0 and second around any frequency ω.

5.2.1. Analysis around the real frequency ω_0

Numerical solutions are performed assuming that the frequency ω is near the real frequency ω_0 as described in Sections 3.2 and 4.1. For each core material cited above, the linear equivalent frequencies and associated loss factors obtained by

Table 4
Nonlinear coefficients associated to the first two vibration modes of the sandwich beam for different core's loss factors.

η_c	RM/IRM		ACM/ECM	
	C^R	C^I	C^R	C^I
Simply supported				
0.1	20.83	2.14×10^{-5}	20.81	2.15×10^{-5}
	30.80	5.68×10^{-5}	30.79	5.68×10^{-5}
0.6	20.83	2.14×10^{-5}	20.21	2.19×10^{-5}
	30.80	5.68×10^{-5}	30.63	5.69×10^{-5}
1	20.83	2.14×10^{-5}	19.25	2.28×10^{-5}
	30.80	5.68×10^{-5}	30.34	5.71×10^{-5}
1.5	20.83	2.14×10^{-5}	17.77	2.44×10^{-5}
	30.80	5.68×10^{-5}	29.80	5.75×10^{-5}
Clamped–clamped				
0.1	7.34	1.40×10^{-5}	7.34	1.40×10^{-5}
	18.54	6.15×10^{-5}	18.54	6.15×10^{-5}
0.6	7.34	1.40×10^{-5}	7.30	1.40×10^{-5}
	10.34	6.15×10^{-5}	18.49	6.16×10^{-5}
1	7.34	1.40×10^{-5}	7.22	1.41×10^{-5}
	18.54	6.15×10^{-5}	18.42	6.18×10^{-5}
1.5	7.34	1.40×10^{-5}	7.08	1.42×10^{-5}
	18.54	6.15×10^{-5}	18.28	6.22×10^{-5}
Clamped–simple				
0.1	13.89	1.92×10^{-5}	13.89	1.92×10^{-5}
	27.18	6.72×10^{-5}	27.18	6.72×10^{-5}
0.6	13.89	1.92×10^{-5}	13.67	1.93×10^{-5}
	27.18	6.72×10^{-5}	27.11	6.73×10^{-5}
1	13.89	1.92×10^{-5}	13.30	1.95×10^{-5}
	27.18	6.72×10^{-5}	26.98	6.75×10^{-5}
1.5	13.89	1.92×10^{-5}	12.68	1.99×10^{-5}
	27.18	6.72×10^{-5}	26.74	6.80×10^{-5}

Table 5
Maxwell series terms (39) at 27 °C and 20 °C of 3M ISD112 [1,36].

j	27 °C			20 °C		
	G_0 (Pa)	Δ_j	Ω_j (rad s^{-1})	G_0 (Pa)	Δ_j	Ω_j (rad s^{-1})
1	0.5×10^6	0.746	468.7	0.0511×10^6	2.8164	31.1176
2		3.265	4742.4		13.1162	446.4542
3		43.284	71532.5		45.4655	5502.5318

different eigenmodes approaches are given in Table 6 for the clamped–free sandwich beam and in Table 7 for the clamped–clamped sandwich beam. Results of both tables show that the linear equivalent frequencies and associated loss factors obtained by the ACM approach are very closer to those of the ECM approach whatever the viscoelastic law. The equivalence between both approaches already seen for constant viscoelastic models is one more shown here for frequency dependent models. Results obtained by the RM approach are completely different from those of the ACM and ECM approaches. As already seen for the constant viscoelastic models, the RM approach herein overestimates the equivalent loss factors and the worse case is observed for the PVB viscoelastic law at 20°C where the linear equivalent frequencies and associated loss factors of the RM approach are more than the twice of those of the ACM and ECM approaches. This needs to pay a particular attention to the use of the RM approach which is not suitable for any viscoelastic law. In this way, the RM approach must be improved using the IRM approach as presented in Tables 6 and 7 where the linear equivalent frequencies and associated loss factors of the IRM approach are near those of ACM and ECM approaches.

Fig. 5 displays the eigenmode deflection obtained by the ECM approach for the 3M ISD112 and the PVB viscoelastic laws. Although the real and imaginary part have the same mode shape but differ in the amplitude depending on the viscoelastic law. For instance, the imaginary part of the deflection amplitude for the 3M ISD112 law is larger than the one of the PVB law. This explains why for the linear equivalent loss factors presented in Tables 6 and 7, the damping induced by the 3M ISD112 law is greater than the one induced by the PVB law. The imaginary part of the eigenmode which is commonly disregarded in the RM approach may become larger depending on the viscoelastic law and in such a case needs to be considered.

Table 6
The first four linear equivalent frequencies and associated loss factors of the clamped–free sandwich beam for frequency dependent core materials ($\omega \approx \omega_0$).

RM		IRM		ACM		ECM	
Ω_l (Hz)	η_l	Ω_l (Hz)	η_l	Ω_l (Hz)	η_l	Ω_l (Hz)	η_l
3M ISD112 core 27 °C							
63.74	2.39×10^{-1}	63.38	1.86×10^{-1}	65.04	1.59×10^{-1}	65.34	1.56×10^{-1}
317.33	4.06×10^{-1}	312.34	3.02×10^{-1}	322.47	2.60×10^{-1}	326.08	2.55×10^{-1}
827.62	4.19×10^{-1}	814.19	3.25×10^{-1}	839.97	2.88×10^{-1}	849.49	2.78×10^{-1}
1540.09	3.52×10^{-1}	1523.79	2.91×10^{-1}	1556.38	2.70×10^{-1}	1567.53	2.69×10^{-1}
3M ISD112 core 20 °C							
65.97	7.32×10^{-1}	58.31	3.61×10^{-1}	61.96	2.62×10^{-1}	63.07	1.96×10^{-1}
340.04	3.98×10^{-1}	309.04	2.16×10^{-1}	314.58	1.98×10^{-1}	316.54	1.87×10^{-1}
845.85	2.51×10^{-1}	813.76	1.75×10^{-1}	821.85	1.69×10^{-1}	823.29	1.60×10^{-1}
1562.42	1.26×10^{-1}	1526.99	9.71×10^{-2}	1530.85	9.63×10^{-2}	1530.60	9.48×10^{-2}
PVB core 20 °C							
488.78	2.12×10^{-1}	81.78	1.54×10^{-3}	81.80	1.48×10^{-3}	81.79	1.37×10^{-3}
2082.08	1.55×10^{-1}	503.95	6.12×10^{-3}	504.17	5.98×10^{-3}	504.16	5.43×10^{-3}
4183.69	1.29×10^{-1}	1379.56	1.04×10^{-2}	1380.38	1.02×10^{-2}	1380.34	9.38×10^{-3}
6090.64	1.13×10^{-1}	2626.08	1.48×10^{-2}	2627.92	1.46×10^{-2}	2627.87	1.36×10^{-2}

Table 7
The first four linear equivalent frequencies and associated loss factors of the clamped–clamped sandwich beam for frequency dependent core materials ($\omega \approx \omega_0$).

RM		IRM		ACM		ECM	
Ω_l (Hz)	η_l	Ω_l (Hz)	η_l	Ω_l (Hz)	η_l	Ω_l (Hz)	η_l
3M ISD112 core 27 °C							
288.11	2.91×10^{-1}	286.88	2.59×10^{-1}	291.38	2.47×10^{-1}	292.70	2.49×10^{-1}
774.38	3.05×10^{-1}	768.85	2.61×10^{-1}	781.34	2.46×10^{-1}	784.94	2.45×10^{-1}
1485.64	2.79×10^{-1}	1476.96	2.44×10^{-1}	1492.02	2.34×10^{-1}	1502.34	2.34×10^{-1}
2412.39	2.62×10^{-1}	2401.45	2.34×10^{-1}	2428.93	2.26×10^{-1}	2436.94	2.27×10^{-1}
3M ISD112 core 20 °C							
289.24	2.28×10^{-1}	285.06	1.88×10^{-1}	287.38	1.83×10^{-1}	288.07	1.80×10^{-1}
781.95	1.77×10^{-1}	769.52	1.42×10^{-1}	773.39	1.39×10^{-1}	774.05	1.36×10^{-1}
1494.62	9.70×10^{-2}	1480.16	8.21×10^{-2}	1482.51	8.17×10^{-2}	1482.42	8.09×10^{-2}
2398.41	4.88×10^{-2}	2385.10	4.31×10^{-2}	2386.03	4.31×10^{-2}	2385.94	4.30×10^{-2}
PVB core 20 °C							
1631.84	1.56×10^{-1}	506.46	9.14×10^{-3}	506.79	8.94×10^{-3}	506.77	8.03×10^{-3}
3382.00	1.28×10^{-1}	1357.71	1.38×10^{-2}	1358.75	1.36×10^{-2}	1358.71	1.25×10^{-2}
5280.18	1.11×10^{-1}	2579.46	1.79×10^{-2}	2581.56	1.77×10^{-2}	2581.50	1.65×10^{-2}
7241.05	9.88×10^{-2}	4120.84	2.14×10^{-2}	4124.21	2.12×10^{-2}	4124.14	2.00×10^{-2}

The linear responses corresponding to the first vibration mode of the simply supported and the clamped–free sandwich beam using the 3M ISD112 law at 20 °C are presented in Fig. 6 for different eigenmodes approaches. It is seen that the RM approach underestimates the sandwich beam response compared to the ACM and the ECM approaches. The response is improved when using the IRM approach. Indeed, the responses obtained by the ACM and the ECM approaches are closer. The same observations are raised for the corresponding linear phases presented in Fig. 7 where the phase curves obtained by the RM approach are clearly shifted from those obtained by the ACM and ECM approaches.

For the nonlinear vibrations analysis, the nonlinear modal coefficients associated to the two first vibration modes for frequency dependent models are presented in Table 8 for different eigenmodes approaches. Results obtained by the ACM approach are nearly the same compared to those of the ECM approach. As the nonlinear modal coefficients provided by the RM approach are so far from those of the ACM and ECM approaches especially for the PVB viscoelastic law, there is a need to improve the RM approach which is the proposed IRM approach.

5.2.2. Analysis around any frequency ω

The present analysis is held for frequency dependent models in a general way without any restriction on the frequency by following the generalized approach presented in Section 4.2. The emphasis is the comparison of the three main eigenmodes approaches, i.e: the RM, ACM and ECM approaches in the linear and nonlinear framework. The linear and nonlinear response curves corresponding to the first vibration mode of the simply supported sandwich beam for the 3M

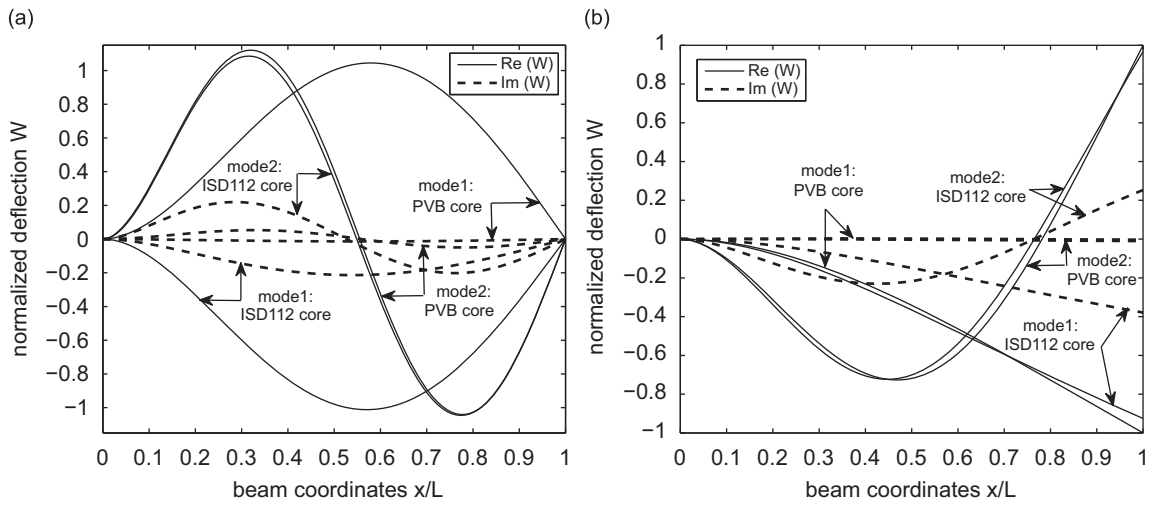

Fig. 5. Real and imaginary parts of the eigenmode deflection of the sandwich beam for different frequency dependent core materials: 3M ISD112 at 27 °C and PVB at 20 °C: (a) C–S beam normalized at $x_0=L/2$ for the first mode and at $x_0=L/4$ for the second mode, (b) C–F beam normalized at $x_0=L$.

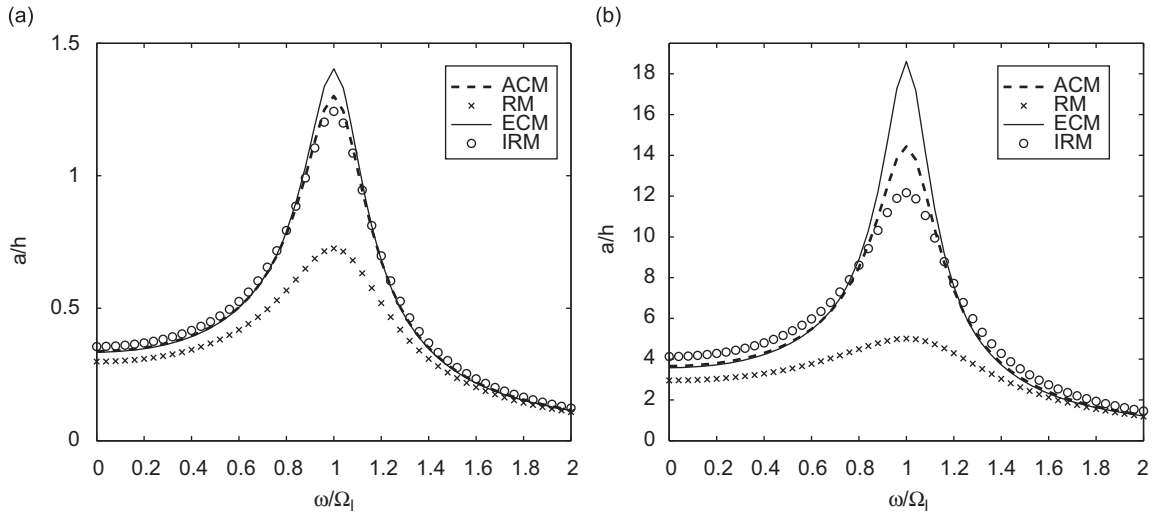

Fig. 6. Linear responses corresponding to the first vibration mode obtained by various eigenmode approaches of the sandwich beam for the 3M ISD112 core at 20 °C under a concentrated force $f=10N$ at $L/2$ for S–S and at L for C–F. (a) Simply supported (S–S): $f(L/2)=10N$, (b) clamped–free (C–F): $f(L)=10N$.

ISD112 viscoelastic law at 20 °C are presented in Figs. 8(a) and (b), respectively. One can realize that the ACM and ECM responses are closer but the RM response is completely shifted from the both. Before the resonance zone, the RM response is upper the ACM and ECM responses but comes down when reaching the resonance zone. The RM approach underestimates the resonance peak and there is a real need to compute the sandwich beam response accurately using the whole complex eigenmode which may be performed using the ACM or ECM approach. Figs. 8(c) and (d) display the corresponding linear and nonlinear phases, respectively. The phase curves performed with the ACM and ECM approaches are closer except the one performed with the RM approach. As seen above for the responses, The RM phase is undervalued compared to the ACM and ECM phases. Fig. 9 displays the linear and nonlinear response and phase curves corresponding to the first vibration mode of the clamped–simple sandwich beam for the 3M ISD112 viscoelastic law at 27 °C. Despite the change in the viscoelastic law and boundary conditions, one can raise up the same observations as made in Fig. 8. Its comes out from the present assessment that for frequency dependent models, the RM approach is no more suitable and may lead to erroneous results of the damping characteristics, phase and harmonic response curves. Complex eigenmodes are needed to establish an efficient Galerkin's basis for linear and nonlinear vibrations analysis of viscoelastic sandwich beams. As the

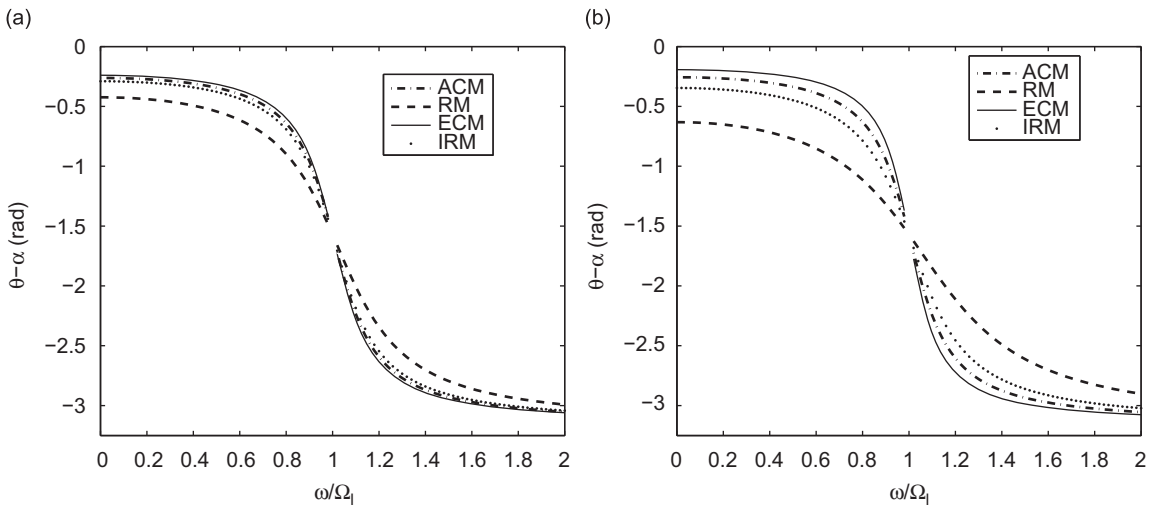

Fig. 7. Linear phases corresponding to the first vibration mode obtained by various eigenmode approaches of the sandwich beam for the 3M ISD112 core at 20 °C. (a) Simply supported (S–S), (b) clamped–free (C–F).

Table 8
Nonlinear coefficients associated to the first two vibration modes of the sandwich beam for frequency dependent core's materials ($\omega \approx \omega_0$).

	RM		IRM		ACM		ECM	
	C^R	C^I	C^R	C^I	C^R	C^I	C^R	C^I
Simply supported								
ISD112 27 °C	18.93	3.48×10^{-5}	19.36	4.48×10^{-5}	18.10	4.75×10^{-5}	17.72	4.70×10^{-5}
	25.67	9.71×10^{-5}	26.16	1.17×10^{-4}	24.69	1.20×10^{-4}	24.01	1.20×10^{-4}
ISD112 20 °C	18.20	1.84×10^{-5}	20.61	3.15×10^{-5}	19.42	3.30×10^{-5}	19.09	3.56×10^{-5}
	25.27	6.65×10^{-5}	26.44	8.80×10^{-5}	25.84	8.90×10^{-5}	25.59	9.22×10^{-5}
PVB 20 °C	0.31	1.86×10^{-5}	8.77	3.58×10^{-2}	8.76	3.70×10^{-2}	8.76	4.09×10^{-2}
	8.09	5.46×10^{-5}	9.09	1.25×10^{-2}	9.08	1.28×10^{-2}	9.08	1.41×10^{-2}
Clamped–clamped								
ISD112 27 °C	6.68	2.54×10^{-5}	6.69	2.85×10^{-5}	6.46	2.89×10^{-5}	6.41	2.85×10^{-5}
	15.94	1.05×10^{-4}	15.88	1.23×10^{-4}	15.28	1.25×10^{-4}	15.12	1.24×10^{-4}
ISD112 20 °C	6.69	1.93×10^{-5}	6.78	2.38×10^{-5}	6.66	2.39×10^{-5}	6.62	2.41×10^{-5}
	15.76	5.87×10^{-5}	15.84	7.37×10^{-5}	15.66	7.42×10^{-5}	15.59	7.55×10^{-5}
PVB 20 °C	0.21	1.35×10^{-5}	2.16	2.36×10^{-3}	2.15	2.41×10^{-3}	2.16	2.68×10^{-3}
	0.84	6.01×10^{-5}	5.06	3.33×10^{-3}	5.06	3.37×10^{-3}	5.07	3.68×10^{-3}
Clamped–simple								
ISD112 27 °C	12.68	3.40×10^{-5}	12.66	4.01×10^{-5}	11.98	4.10×10^{-5}	11.80	4.03×10^{-5}
	23.01	1.15×10^{-4}	22.91	1.34×10^{-4}	21.83	1.37×10^{-4}	21.45	1.36×10^{-4}
ISD112 20 °C	12.57	3.22×10^{-5}	13.03	3.20×10^{-5}	12.57	3.25×10^{-5}	12.43	3.31×10^{-5}
	22.77	7.20×10^{-5}	22.99	9.08×10^{-5}	22.62	9.15×10^{-5}	22.42	9.38×10^{-5}
PVB 20 °C	0.28	1.78×10^{-5}	4.74	8.27×10^{-3}	4.73	8.48×10^{-3}	4.74	9.47×10^{-3}
	0.94	6.54×10^{-5}	7.46	6.65×10^{-3}	7.45	6.75×10^{-3}	7.46	7.42×10^{-3}

present study reveals the equivalence of the ACM and ECM approaches, the complex eigenmodes of the Galerkin's basis may be performed using the ACM approach which is less expensive.

6. Conclusion

A numerical method for linear and nonlinear vibrations analysis of viscoelastic sandwich beams has been developed based on finite element solutions. This method couples the harmonic balance technique to one mode Galerkin's procedure. A general formulation taking into account the complex constant and the frequency dependent viscoelastic models has been developed.

Four numerical models for eigenmodes computation have been proposed to establish the Galerkin's basis: real eigenmodes (RM), improved real eigenmodes (IRM), approached complex eigenmodes (ACM) and exact complex

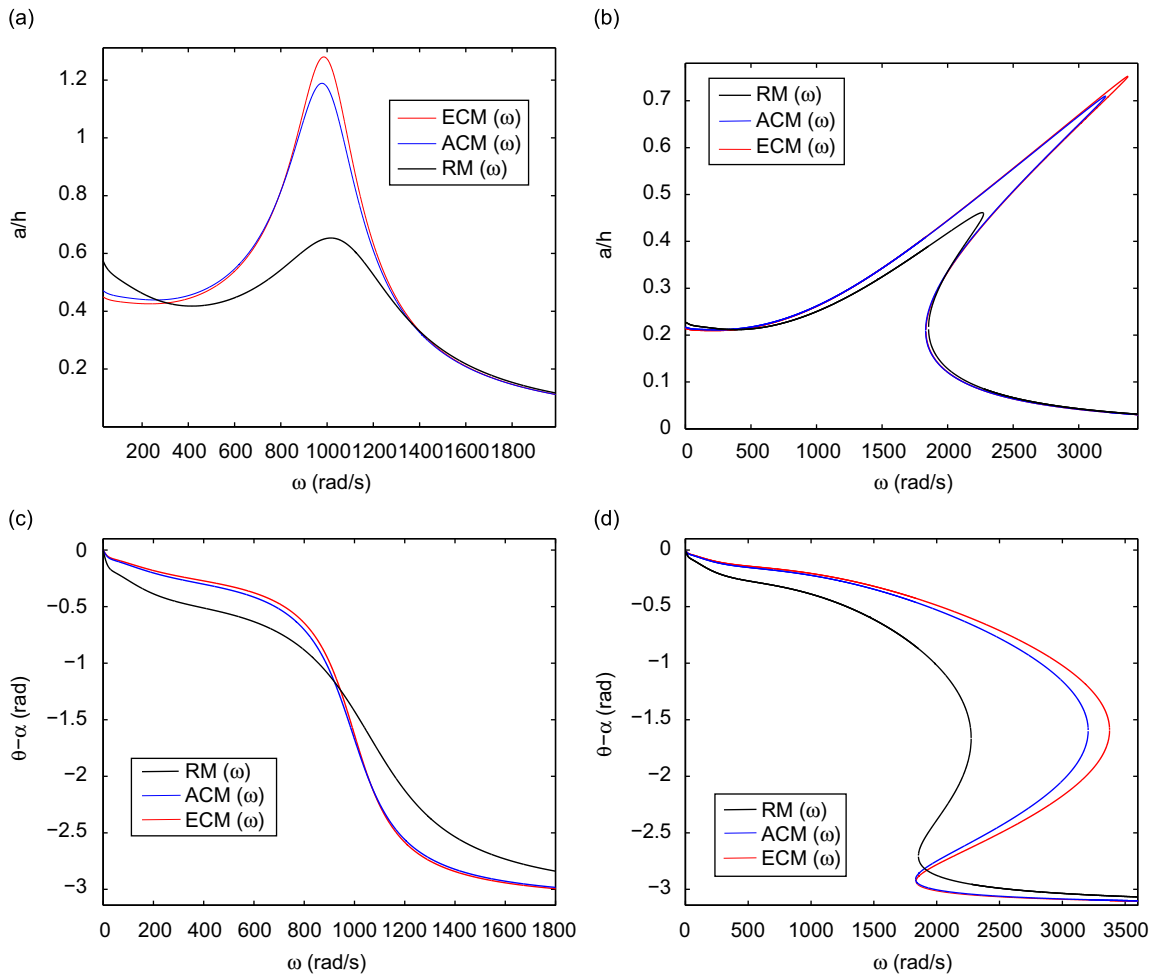

Fig. 8. Linear and nonlinear response and phase curves corresponding to the first vibration mode of the S–S sandwich beam with frequency dependent 3M ISD112 core at 20 °C associated to various eigenmode approaches, concentrated excitation force $f=10N$ at $L/2$. (a) Linear response, (b) nonlinear response, (c) linear phase and (d) nonlinear phase.

eigenmodes (ECM). The analysis has been conducted first in a simple framework and second in a general one for various viscoelastic laws and boundary conditions. To raise a clear picture on the validity and accuracy of the classical RM approach, a numerical assessment has been held based on the linear and nonlinear vibrations characteristics and on the harmonic response and phase curves performed with each eigenmode approach. The obtained results show that for the constant viscoelastic models:

- the RM and IRM approaches are exactly the same,
- the ACM and ECM approaches are exactly the same,
- the RM approach is well efficient and accurate only for small damping but leads to erroneous results for high damping.

For the frequency dependent models, the obtained results show that:

- the ACM approach is equivalent to the ECM approach,
- the RM approach leads to erroneous results which may be improved using the IRM approach.

It comes out from the present assessment a misstrust in the use of real eigenmodes as Galerkin's basis, especially for frequency dependent models. Therefore, complex eigenmodes are needed to establish an efficient Galerkin's basis for an accurate modeling of the linear and nonlinear vibrations of viscoelastic sandwich structures. As the present study reveals the equivalence between the ACM and ECM approaches, the complex eigenmodes of the Galerkin's basis may be performed using the ACM approach which is less expensive. Future work is concerned with complex multimodes approach and nonlinear vibration modeling of viscoelastic plates and shells.

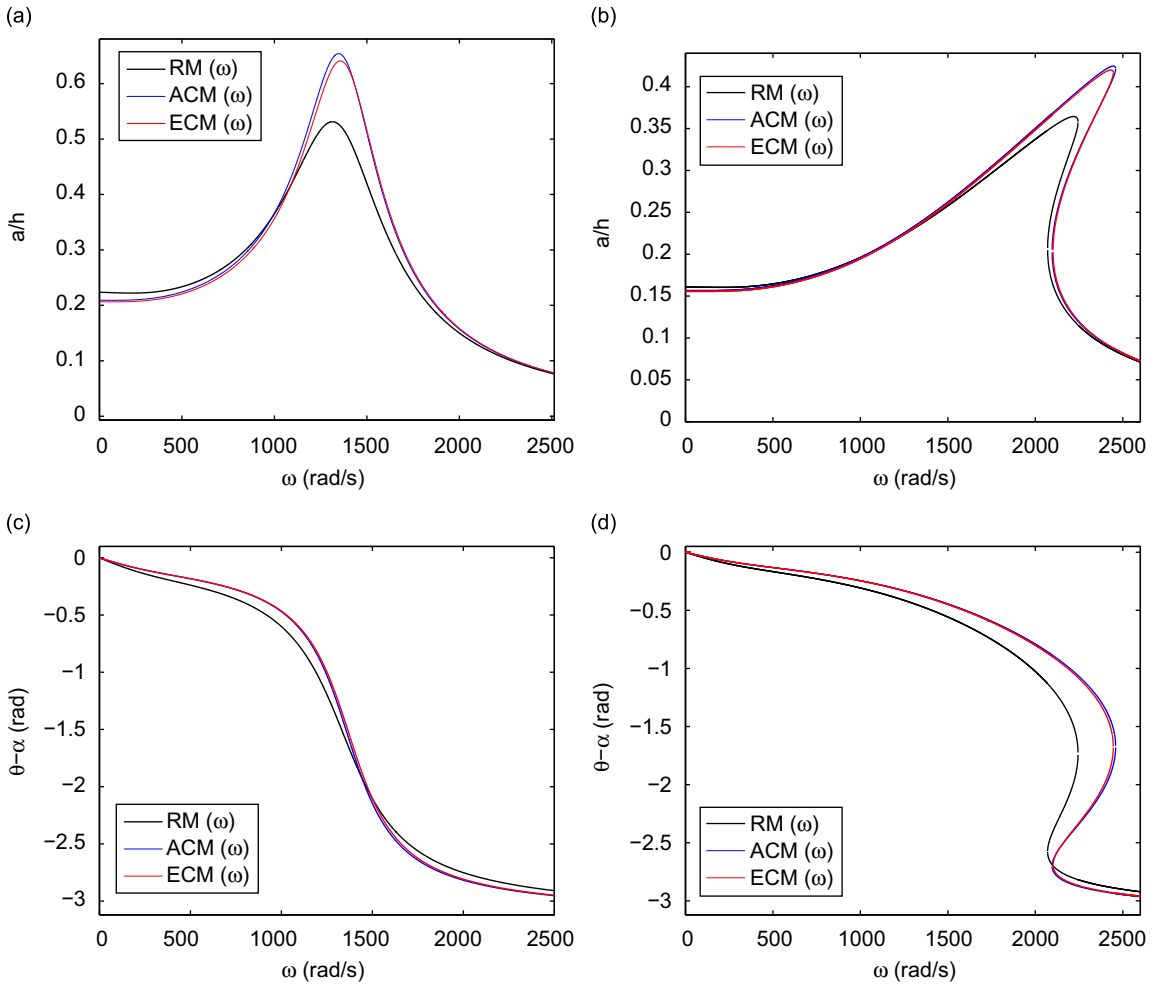

Fig. 9. Linear and nonlinear response and phase curves corresponding to the first vibration mode of the C–S sandwich beam with frequency dependent 3M ISD112 core at 27 °C associated to various eigenmode approaches, concentrated excitation force f=10N at $L/2$. (a) Linear response, (b) nonlinear response, (c) linear phase and (d) nonlinear phase.

Appendix A. Strain, displacement field and constitutive laws

Based on the kinematic model as described in Section 2.1, the strain and displacement fields are presented for the face layers i=1,3:

$$U_i(x,z,t) = u_i(x,t) - (z-z_i)\frac{\partial w}{\partial x}$$

$$W_i(x,z,t) = w(x,t)$$

$$\varepsilon_i(x,z,t) = \frac{\partial u_i}{\partial x} + \frac{1}{2}\left(\frac{\partial w}{\partial x}\right)^2 - (z-z_i)\frac{\partial^2 w}{\partial x^2} \tag{41}$$

where $z_1 = (h_f + h_c)/2 = -z_3$, u_i represents the axial displacement of the middle surface of the ith layer and w the common transverse displacement. Those related to the viscoelastic layer i=2 are

$$U_2(x,z,t) = u(x,t) + z\beta(x,t)$$

$$W_2(x,z,t) = w(x,t)$$

$$\varepsilon_2(x,z,t) = \frac{\partial u}{\partial x} + \frac{1}{2}\left(\frac{\partial w}{\partial x}\right)^2 + z\frac{\partial \beta}{\partial x}$$

$$\xi_2(x,z,t) = \beta + \frac{\partial w}{\partial x} \tag{42}$$

where u and β are, respectively, the axial displacement of the middle surface and the rotation of the normal to the middle plane of the viscoelastic core. ε_2 is the normal strain and ξ_2 the shear strain of the viscoelastic core. The displacements continuity assumptions at the interfaces between the three layers result in the following relations:

$$u_1 = u + \left[\frac{h_c}{2}\beta - \frac{h_f}{2}\frac{\partial w}{\partial x}\right]$$

$$u_3 = u - \left[\frac{h_c}{2}\beta - \frac{h_f}{2}\frac{\partial w}{\partial x}\right] \tag{43}$$

Based on the generalized Hooke's stress–strain law, the constitutive behavior of the sandwich beam is expressed through the axial force N_i and bending moment M_i of each layer i:

$$N_i(x,t) = E_f S_f \left[\frac{\partial u_i}{\partial x} + \frac{1}{2}\left(\frac{\partial w}{\partial x}\right)^2\right] \quad i = 1,3$$

$$M_i(x,t) = E_f I_f \frac{\partial^2 w}{\partial x^2} \tag{44}$$

where E_f denotes the Young's modulus of the face layers, S_f and I_f represent the area and the quadratic moment of the faces cross-section, respectively. The axial force and bending moment in the viscoelastic layer i=2 are given in form of convolution product:

$$N_2(x,t) = S_c Y(t) * \frac{\partial}{\partial t}\left[\frac{\partial u}{\partial x} + \frac{1}{2}\left(\frac{\partial w}{\partial x}\right)^2\right]$$

$$M_2(x,t) = I_c Y(t) * \frac{\partial}{\partial t}\left(\frac{\partial \beta}{\partial x}\right) \tag{45}$$

where S_c and I_c are the area and the quadratic moment of the cross-section of the viscoelastic core, respectively. $Y(t)$ denotes the relaxation function and v_c the Poisson ratio of the viscoelastic core material. The shear force induced in the viscoelastic layer is

$$T(x,t) = \frac{S_c}{2(1+v_c)} Y(t) * \frac{\partial}{\partial t}\left(\frac{\partial w}{\partial x} + \beta\right) \tag{46}$$

Appendix B. Element matrices and shape functions

Denoting by L^e the element length and setting $\xi = 2x/L^e - 1$, for $x \in [0\ L^e]$ and $\xi \in [-1\ 1]$, the classical polynomial shape functions used in Section 3.1 are defined in [20] as

$$n_1(\xi) = \frac{(1-\xi)^2(2+\xi)}{4}$$

$$n_2(\xi) = \frac{L^e(1-\xi)^2(1+\xi)}{8}$$

$$n_3(\xi) = \frac{(1+\xi)^2(2-\xi)}{4}$$

$$n_4(\xi) = -\frac{L^e(1+\xi)^2(1-\xi)}{8}$$

$$n_5(\xi) = \frac{1-\xi}{2}$$

$$n_6(\xi) = \frac{1+\xi}{2} \tag{47}$$

The element mass and stiffness matrices used in Section 3.1 are expressed as:

$$[M^e] = (2\rho_f S_f + \rho_c S_c)[m^e]$$

$$[K^e] = \tfrac{1}{2}\{(2I_c E_c(\omega) + E_f S_f h_c^2)[k_1^e] - E_f S_f h_f h_c [k_2^e]\} + \tfrac{1}{2}\{E_f(4I_f + S_f h_f^2)[k_3^e] + 2S_c G_c(\omega)[k_4^e]\} \tag{48}$$

$$[m^e] = \int_{-1}^{1} J^T [N_w][N_w]\, \mathrm{d}\xi$$

$$[k_1^e] = \int_{-1}^{1} J^{-1^T}[N'_\beta][N'_\beta]\,\mathrm{d}\xi$$

$$[k_2^e] = \int_{-1}^{1} J^{-2}({}^T[N'_\beta][N''_w] + {}^T[N''_w][N'_\beta])\,\mathrm{d}\xi$$

$$[k_3^e] = \int_{-1}^{1} J^{-3^T}[N''_w][N''_w]\,\mathrm{d}\xi$$

$$[k_4^e] = \int_{-1}^{1} (J^{-1^T}[N'_w][N'_w] + {}^T[N_\beta][N'_w] + {}^T[N'_w][N_\beta] + J^T[N_\beta][N_\beta])\,\mathrm{d}\xi \tag{49}$$

where $J=L^e/2$ and the notations $[X']$, $[X'']$ stand for the first and the second derivatives of the matrix $[X(\xi)]$ with respect to ξ.

Appendix C. Reduced equations for axially immovable ends

Integrating Eq. (23) for immovable ends $u(0)=u(L)=0$, one gets

$$u_0(x) = \frac{x}{L}\int_0^L |W'(s)|^2\,\mathrm{d}s - \int_0^x |W'(s)|^2\,\mathrm{d}s$$

$$u_{2\omega}(x) = \frac{x}{2L}\int_0^L (W'(s))^2\,\mathrm{d}s - \int_0^x \frac{1}{2}(W'(s))^2\,\mathrm{d}s \tag{50}$$

Using Eq. (50) in Eq. (22) the amplitudes of the axial force are given by

$$N_0(x) = \frac{2E_fS_f + S_cE_c(0)}{L}\int_0^L |W'(s)|^2\,\mathrm{d}s$$

$$N_{2\omega}(x) = \frac{2E_fS_f + S_cE_c(2\omega)}{2L}\int_0^L (W'(s))^2\,\mathrm{d}s \tag{51}$$

Thus, the nonlinear modal stiffness appearing in Eq. (25) is

$$k_{nl} = \frac{2E_fS_f + S_cE_c(0)}{L}\left(\int_0^L |W'(x)|^2\,\mathrm{d}x\right)^2 + \frac{2E_fS_f + S_cE_c(2\omega)}{2L}\left|\int_0^L (W'(x))^2\,\mathrm{d}x\right|^2 \tag{52}$$

It is not difficult to compute k_{nl} since the deflection $W(x)$ is discretized using the finite element model proposed in Section 3.1, see Eq. (9a). Denoting by $[k_5]$ the matrix obtained when assembling the element matrix $[k_5^e] = \int_{-1}^{1} J^{-1^T}[N'_w][N'_w]\,\mathrm{d}\xi$, the integrations related to k_{nl} are given by

$$\int_0^L |W'(x)|^2\,\mathrm{d}x = {}^T\{\overline{U}\}[k_5]\{U\}$$

$$\int_0^L (W'(x))^2\,\mathrm{d}x = {}^T\{U\}[k_5]\{U\} \tag{53}$$

where the matrix $[N'_w]$ represents the derivative of the matrix $[N_w]$ with respect to ξ.

References

[1] M. Trindade, A. Benjeddou, R. Ohayon, Modeling of frequency dependent viscoelastic materials for active–passive vibration damping, *Journal of Vibration and Acoustics* 122 (2) (2000) 169–174.

[2] M. Haberman, Design of High Loss Viscoelastic Composites Through Micromechanical Modeling and Decision Based Material by Design, PhD Thesis, George W. Woodruff School of Mechanical Engineering, Atlanta, 2007.

[3] H. Hu, S. Belouettar, M. Potier-Ferry, E.M. Daya, Review and assessment of various theories for modeling sandwich composites, *Composite Structures* 84 (3) (2008) 282–292.

[4] E.M. Daya, M. Potier-Ferry, A numerical method for nonlinear eigenvalue problems application to vibrations of viscoelastic structures, *Computers and Structures* 79 (5) (2001) 533–541.

[5] L. Azrar, R. Benamar, R.G. White, A semi-analytical approach to the nonlinear dynamic response problem of beams at large vibration amplitudes, part II: multimode approach to the steady state forced periodic response, *Journal of Sound and Vibration* 255 (1) (2002) 1–41.

[6] A. Przekop, M.S. Azzouz, X. Guo, C. Mei, L. Azrar, Finite element multimode approach to nonlinear free vibrations of shallow shells, *American Institute of Aeronautics and Astronautics Journal* 42 (11) (2004) 2373–2381.

[7] L. Azrar, R. Benamar, M. Potier-Ferry, An asymptotic numerical method for large-amplitude free vibrations of thin elastic plates, *Journal of Sound and Vibration* 220 (1999) 695–727.

[8] L. Azrar, E. Boutyour, M. Potier-Ferry, Nonlinear forced vibrations of plates by an asymptotic-numerical method, *Journal of Sound and Vibration* 252 (2002) 657–674.

[9] R. Arquier, S. Bellizzi, R. Bouc, B. Cochelin, Two methods for the computation of nonlinear modes of vibrating systems at large amplitudes, *Computers and Structures* 84 (2006) 1565–1576.

[10] E.J. Kovac, W. Anderson, R. Scott, Forced nonlinear vibrations of damped sandwich beam, *Journal of Sound and Vibration* 17 (1) (1971) 25–39.

[11] M. Hyer, W. Anderson, R. Scott, Nonlinear vibrations of three-layer beams with viscoelastic core i: theory, *Journal of Sound and Vibration* 46 (1) (1976) 121–136.
[12] V.P. Iu, Y. Cheung, S. Lau, Nonlinear vibration analysis of multilayer beams by incremental finite elements, part I: theory and numerical formulation, *Journal of Sound and Vibration* 100 (3) (1985) 359–372.
[13] V.P. Iu, Y.K. Cheung, S. Lau, Nonlinear vibration analysis of multilayer beams by incremental finite elements, p art II: damping and forced vibrations, *Journal of Sound and Vibration* 100 (3) (1985) 373–382.
[14] Z.Q. Xia, S. Lukasiewicz, Nonlinear, free, damped vibrations of sandwich plates, *Journal of Sound and Vibration* 175 (2) (1994) 219–232.
[15] Z.Q. Xia, S. Lukasiewicz, Nonlinear analysis of damping properties of cylindrical sandwich panels, *Journal of Sound and Vibration* 186 (1) (1995) 55–69.
[16] M. Ganapathi, B.P. Patel, P. Boisse, O. Polit, Flexural loss factors of sandwich and laminated composite beams using linear and nonlinear dynamic analysis, *Composites Part B: Engineering* 30 (3) (1999) 245–256.
[17] E.M. Daya, L. Azrar, M. Potier-Ferry, An amplitude equation for the nonlinear vibration of viscoelastically damped sandwich beams, *Journal of Sound and Vibration* 271 (3–5) (2004) 789–813.
[18] E.M. Daya, L. Azrar, M. Potier-Ferry, Modélisation par éléments finis des vibrations non-linéaires des plaques sandwich viscoélastiques, *Mécanique & Industries* 6 (2005) 13–20.
[19] E. Boutyour, E. Daya, L. Azrar, M. Potier-Ferry, An approximated harmonic balance method for nonlinear vibration of viscoelastic structures, *Journal of Engineering Materials and Technology* 128 (3) (2006) 330–334.
[20] G. Dhatt, G. Touzot, Une présentation de la méthode des éléments finis, Maloine S.A. 2ème édition, 1984.
[21] B. Ma, J. He, A finite element analysis of viscoelastically damped sandwich plates, *Journal of Sound and Vibration* 152 (1) (1992) 107–123.
[22] L. Duigou, E.M. Daya, M. Potier-Ferry, Iterative algorithms for nonlinear eigenvalue problems. Application to vibrations of viscoelastic shells, *Computer Methods in Applied Mechanics and Engineering* 192 (2003) 1323–1335.
[23] X. Chen, H.L. Chen, X.L. Hu, Damping prediction of sandwich structures by order-reduction-iteration approach, *Journal of Sound and Vibration* 222 (5) (1999) 803–812.
[24] E.E. Ungar, E.M. Kerwin, Loss factors of viscoelastic systems in terms of energy concepts, *The Journal of the Acoustical Society of America* 34 (7) (1962) 954–957.
[25] M.L. Soni, Finite element analysis of viscoelastically damped sandwich structures, *Shock and Vibration Bulletin* 55 (1) (1981) 97–109.
[26] R. Rickards, A. Chate, E. Barkanov, Finite element analysis of damping the vibrations of laminated composites, *Computers and Structures* 47 (6) (1993) 1005–1015.
[27] J. Wilkinson, *The Algebraic Eigenvalue Problem*, Clarendon Press, Oxford, 1965.
[28] H. Voss, An Arnoldi method for nonlinear eigenvalue problems, *BIT Numerical Mathematics* 444 (2004) 387–401.
[29] I. Charpentier, M. Potier-Ferry, Différentiation automatique de la méthode asymptotique numérique typée: l'approche Diamant, *C. R. Mécanique* 336 (2008) 336–340.
[30] Y. Koutsawa, I. Charpentier, E.M. Daya, M. Cherkaoui, A generic approach for the solution of nonlinear residual equations. Part I: the Diamant toolbox, *Computer Methods in Applied Mechanics and Engineering* 198 (3–4) (2008) 572–577.
[31] M. Bilasse, I. Charpentier, E.M. Daya, Y. Koutsawa, A generic approach for the solution of nonlinear residual equations. Part II: homotopy and complex nonlinear eigenvalue method, *Computer Methods in Applied Mechanics and Engineering* 198 (2009) 3999–4004.
[32] E. Mallil, H. Lahmam, N. Damil, M. Potier-Ferry, An iterative process based on homotopy and perturbation techniques, *Computer Methods in Applied Mechanics and Engineering* 190 (2000) 1845–1858.
[33] S.H. Hoseini, T. Pirbodaghi, M. Asghari, G.H. Farrahi, M.T. Ahmadian, Nonlinear free vibration of conservative oscillators with inertia and static type cubic nonlinearities using homotopy analysis method, *Journal of Sound and Vibration* 316 (2008) 263–273.
[34] F. Abdoun, L. Azrar, E. Daya, M. Potier-Ferry, Forced harmonic response of viscoelastic structures by an asymptotic numerical method, *Computers and Structures* 87 (2009) 91–100.
[35] D. Rao, Frequency and loss factors of sandwich beams under various boundary conditions, *Mechanical Engineering Science* 20 (1978) 271–282.
[36] M.A. Trindade, Reduced-order finite element models of viscoelastically damped beams through internal variables projection, *Journal of Vibration and Acoustics* 128 (2006) 501–508.